Solutions to Problems 1

98

Chuizheng Kong

October 18, 2024

1

1.1

1.1.1

Show that the mean square velocity for a Maxwellian distribution is

$$\langle v^2 \rangle = \frac{3k_\mathrm{B}T}{m} \tag{1.1.1}$$

Proof: The Maxwell-Boltzmann distribution for the speed v of particles with mass m at temperature T is:

$$f(v) = 4\pi \left(\frac{m}{2\pi k_\mathrm{B} T} \right)^{3/2} v^2 e^{-\frac{mv^2}{2k_\mathrm{B}T}} \tag{1.1.2}$$

The mean square velocity is:

$$\langle v^2 \rangle = \int_0^{+\infty} v^2 f(v) \mathrm{d}v \tag{1.1.3}$$

Plugging in the expression for $f(v)$ and calculating the integral, we find:

$$\begin{aligned} \langle v^2 \rangle &= 4\pi \left(\frac{m}{2\pi k_\mathrm{B} T} \right)^{3/2} \int_0^{+\infty} v^4 e^{-\frac{mv^2}{2k_\mathrm{B}T}} \mathrm{d}v \\ &= 4\pi \left(\frac{m}{2\pi k_\mathrm{B} T} \right)^{3/2} 2^{3/2} \left(\frac{k_\mathrm{B}T}{m} \right)^{5/2} \int_0^{+\infty} x^{3/2} e^{-x} \mathrm{d}x \\ &= \frac{4k_\mathrm{B}T}{\sqrt{\pi} m} \Gamma\left(\frac{5}{2} \right) = \frac{3k_\mathrm{B}T}{m} \end{aligned} \tag{1.1.4}$$

1.1.2

Show that for gas particles A and B in thermal and kinetic equilibrium at temperature T, the distribution function for the relative speed $v = |\boldsymbol{v}_\mathrm{A} - \boldsymbol{v}_\mathrm{B}|$ in encounters between A and B is given by a Maxwellian velocity distribution

$$f(v)\mathrm{d}v = 4\pi \left(\frac{\mu}{2\pi k_\mathrm{B} T} \right)^{3/2} e^{-\frac{\mu v^2}{2k_\mathrm{B}T}} v^2 \mathrm{d}v \tag{1.1.5}$$

where $\mu = \dfrac{m_\mathrm{A} m_\mathrm{B}}{m_\mathrm{A} + m_\mathrm{B}}$ is the reduced mass.

Proof: The velocity components of particles A and B are independently distributed according to the Maxwell-Boltzmann distribution ($i = x, y, z$):

$$f_\mathrm{A}(v_{\mathrm{A}i}) = \sqrt{\frac{m_\mathrm{A}}{2\pi k_\mathrm{B} T}} e^{-\frac{m_\mathrm{A} v_{\mathrm{A}i}^2}{2k_\mathrm{B} T}} \tag{1.1.6}$$

$$f_\mathrm{B}(v_{\mathrm{B}i}) = \sqrt{\frac{m_\mathrm{B}}{2\pi k_\mathrm{B} T}} e^{-\frac{m_\mathrm{B} v_{\mathrm{B}i}^2}{2k_\mathrm{B} T}} \tag{1.1.7}$$

The components of the relative velocity $\boldsymbol{v} = \boldsymbol{v}_\mathrm{A} - \boldsymbol{v}_\mathrm{B}$ follow the probability distribution function of a linear combination of 2 independent variables:

$$\begin{aligned}
f(v_i) &= \int_{-\infty}^{+\infty} f_\mathrm{A}(v_{\mathrm{A}i}) f_\mathrm{B}(v_{\mathrm{A}i} - v_i) \mathrm{d}v_{\mathrm{A}i} \\
&= \frac{\sqrt{m_\mathrm{A} m_\mathrm{B}}}{2\pi k_B T} \int_{-\infty}^{+\infty} e^{-\frac{m_\mathrm{A} v_{\mathrm{A}i}^2}{2k_\mathrm{B} T}} e^{-\frac{m_\mathrm{B}(v_{\mathrm{A}i} - v_i)^2}{2k_\mathrm{B} T}} \mathrm{d}v_{\mathrm{A}i} \\
&= \frac{\sqrt{m_\mathrm{A} m_\mathrm{B}}}{2\pi k_B T} e^{-\frac{\mu v_i^2}{2k_\mathrm{B} T}} \int_{-\infty}^{+\infty} e^{-\frac{m_\mathrm{A} + m_\mathrm{B}}{2k_\mathrm{B} T}\left(v_{\mathrm{A}i} - \frac{m_\mathrm{B} v_i}{m_\mathrm{A} + m_\mathrm{B}}\right)^2} \mathrm{d}v_{\mathrm{A}i} \\
&= \frac{\sqrt{m_\mathrm{A} m_\mathrm{B}}}{2\pi k_B T} e^{-\frac{\mu v_i^2}{2k_\mathrm{B} T}} \sqrt{\frac{2k_B T}{m_\mathrm{A} + m_\mathrm{B}}} \int_{-\infty}^{+\infty} e^{-x^2} \mathrm{d}x \\
&= \sqrt{\frac{\mu}{2\pi k_B T}} e^{-\frac{\mu v_i^2}{2k_\mathrm{B} T}}
\end{aligned} \tag{1.1.8}$$

Adopt spherical coordinates and integrate the velocities over different directions:

$$\begin{aligned}
f(v)\mathrm{d}v &= \int\int f(v_x) f(v_y) f(v_z) v^2 \sin\theta \mathrm{d}v \mathrm{d}\theta \mathrm{d}\varphi \\
&= \left(\frac{\mu}{2\pi k_\mathrm{B} T}\right)^{3/2} e^{-\frac{\mu(v_x^2 + v_y^2 + v_z^2)}{2k_\mathrm{B} T}} v^2 \mathrm{d}v \int_0^\pi \sin\theta \mathrm{d}\theta \int_0^{2\pi} \mathrm{d}\varphi \\
&= 4\pi \left(\frac{\mu}{2\pi k_\mathrm{B} T}\right)^{3/2} e^{-\frac{\mu v^2}{2k_\mathrm{B} T}} v^2 \mathrm{d}v
\end{aligned} \tag{1.1.9}$$

1.1.3

Compute the total thermal velocities of a proton and an electron at 10^4 K.

Solution: We define the thermal velocity, v_th, as the root mean square of the total velocity:

$$v_\mathrm{th} = \sqrt{\langle v^2 \rangle} = \sqrt{\frac{3k_\mathrm{B} T}{m}} \tag{1.1.10}$$

For a proton or an electron, the thermal velocity is given by:

$$v_{\mathrm{th},p} = \sqrt{\frac{3k_\mathrm{B} T}{m_p}} \approx 1.574 \times 10^4 \text{ m/s} \tag{1.1.11}$$

$$v_{\mathrm{th},e} = \sqrt{\frac{3k_\mathrm{B} T}{m_e}} \approx 6.743 \times 10^5 \text{ m/s} \tag{1.1.12}$$

The total thermal velocities of a proton and an electron at 10^4 K is:

$$v_{\mathrm{th},p} + v_{\mathrm{th},e} \approx 6.900 \times 10^5 \text{ m/s} \tag{1.1.13}$$

1.2

The cooling for the low-temperature ISM is dominated by the following processes (assuming the C and O abundances measured in the local ISM):

(1) [C II] 158μm cooling with free electrons:

$$\frac{\Lambda^{e}_{\rm CII}}{10^{-27}{\rm erg\ cm^3\ s^{-1}}} \approx 3.1 \left(\frac{x}{10^{-3}}\right) \left(\frac{T}{100{\rm K}}\right)^{-0.5} e^{-91.2{\rm K}/T} \tag{1.2.1}$$

(2) [C II] 158μm cooling with hydrogen atoms:

$$\frac{\Lambda^{\rm H}_{\rm CII}}{10^{-27}{\rm erg\ cm^3\ s^{-1}}} \approx 5.2 \left(\frac{T}{100{\rm K}}\right)^{0.13} e^{-91.2{\rm K}/T} \tag{1.2.2}$$

(3) [O I] 63μm cooling with hydrogen atoms:

$$\frac{\Lambda^{\rm H}_{\rm OI}}{10^{-27}{\rm erg\ cm^3\ s^{-1}}} \approx 4.1 \left(\frac{T}{100{\rm K}}\right)^{0.42} e^{-228{\rm K}/T} \tag{1.2.3}$$

(4) Lyman-α (Lyα) cooling with free electrons:

$$\frac{\Lambda^{e}_{{\rm Ly}\alpha}}{10^{-27}{\rm erg\ cm^3\ s^{-1}}} \approx 6 \times 10^5 \left(\frac{x}{10^{-3}}\right) \left(\frac{T}{10^4{\rm K}}\right)^{-0.5} e^{-1.18\times10^5{\rm K}/T} \tag{1.2.4}$$

1.2.1

Reproduce the net cooling function for fractional ionization $x = 10^{-3}$ in the temperature range [10 K, 20000 K].

Solution: The net cooling function $\Lambda(x,T)$ can be calculated by summing the contributions from the different individual cooling processes provided:

$$\begin{aligned}\frac{\Lambda(x,T)}{10^{-27}{\rm erg\ cm^3\ s^{-1}}} &= \frac{\Lambda^{e}_{\rm CII} + \Lambda^{\rm H}_{\rm CII} + \Lambda^{\rm H}_{\rm OI} + \Lambda^{e}_{{\rm Ly}\alpha}}{10^{-40}{\rm J\ m^3\ s^{-1}}} \\ &\approx 3.1 \left(\frac{x}{10^{-3}}\right) \left(\frac{T}{100{\rm K}}\right)^{-0.5} e^{-91.2{\rm K}/T} + 5.2 \left(\frac{T}{100{\rm K}}\right)^{0.13} e^{-91.2{\rm K}/T} \\ &+ 4.1 \left(\frac{T}{100{\rm K}}\right)^{0.42} e^{-228{\rm K}/T} + 6 \times 10^5 \left(\frac{x}{10^{-3}}\right) \left(\frac{T}{10^4{\rm K}}\right)^{-0.5} e^{-1.18\times10^5{\rm K}/T}\end{aligned} \tag{1.2.5}$$

For fractional ionization $x = 10^{-3}$, use $x = 10^{-3}$ in the expression for $\Lambda(x,T)$:

$$\begin{aligned}\frac{\Lambda(x,T)}{10^{-40}{\rm J\cdot m^3\cdot s^{-1}}} &\approx 3.1 \left(\frac{T}{100{\rm K}}\right)^{-0.5} e^{-91.2{\rm K}/T} + 4.1 \left(\frac{T}{100{\rm K}}\right)^{0.42} e^{-228{\rm K}/T} \\ &+ 4.1 \left(\frac{T}{100{\rm K}}\right)^{0.42} e^{-228{\rm K}/T} + 6 \times 10^5 \left(\frac{T}{10^4{\rm K}}\right)^{-0.5} e^{-1.18\times10^5{\rm K}/T}\end{aligned} \tag{1.2.6}$$

Plot the individual cooling rates, as well as the net cooling function, as functions of temperature over the range [10 K, 20,000 K] (see Figure 1).

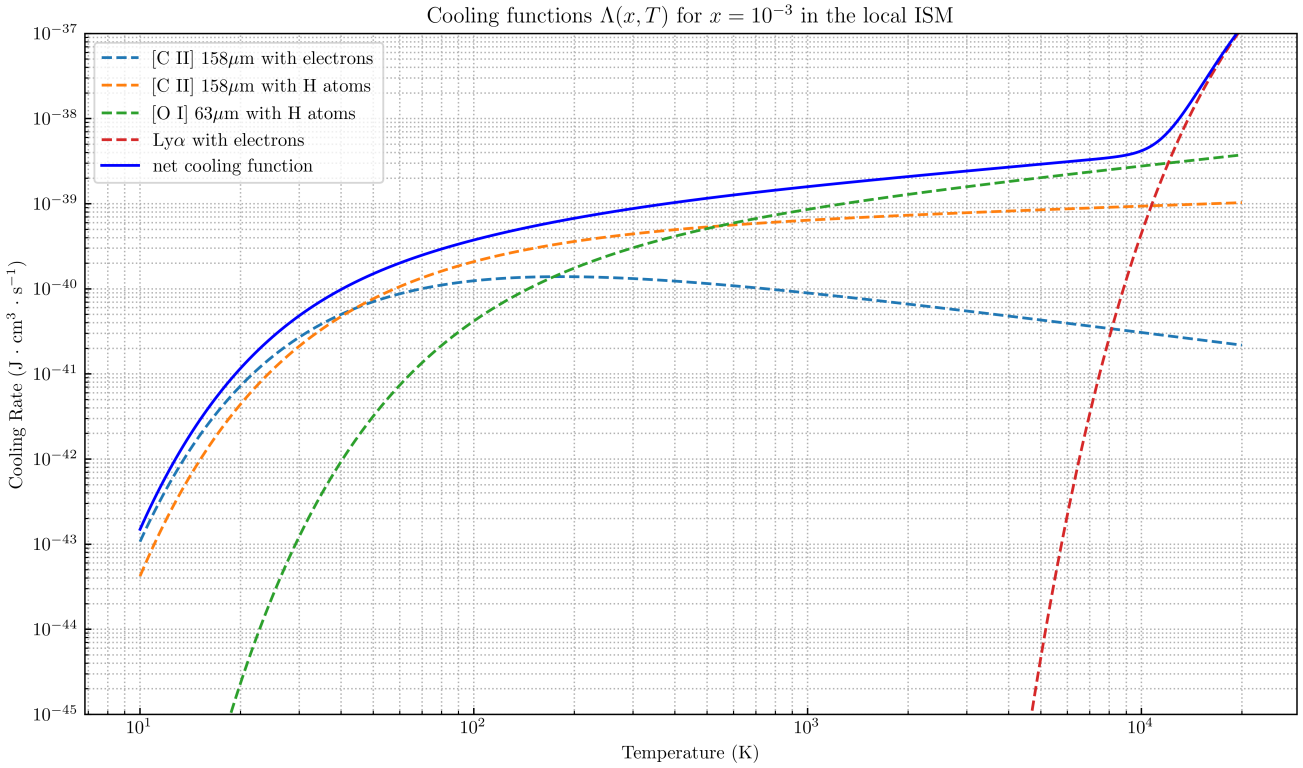

Figure 1: Cooling functions $\Lambda(x,T)$ for $x = 10^{-3}$ in the local ISM

1.2.2

Plot the net cooling function for the C and O abundances that are 10% of those in the local ISM (roughly those in the Small Magellanic Cloud).

Solution: We reduce the cooling contributions from processes involving C and O by a factor of 10%:

$$\frac{\Lambda_{\rm low-metal}(x,T)}{10^{-40}{\rm J\cdot m^3\cdot s^{-1}}} \approx 0.31\left(\frac{T}{100{\rm K}}\right)^{-0.5} e^{-91.2{\rm K}/T} + 0.41\left(\frac{T}{100{\rm K}}\right)^{0.42} e^{-228{\rm K}/T} + 0.41\left(\frac{T}{100{\rm K}}\right)^{0.42} e^{-228{\rm K}/T} + 6\times10^5\left(\frac{T}{10^4{\rm K}}\right)^{-0.5} e^{-1.18\times10^5{\rm K}/T} \tag{1.2.7}$$

Plot again (see Figure 2).

1.2.3

Now consider the heating and cooling balance in this low-metallicity ISM by assuming the dominant heating process is photoelectric heating by dust $\Gamma \approx 2\times10^{-26}$ erg/s. Plot the curve of the equilibrium density $n(T)$ in the density-temperature plane.

Solution: At thermal equilibrium, heating equals cooling:

$$\Gamma = n(T)\Lambda_{\rm low-metal}(x,T) \tag{1.2.8}$$

Solve for equilibrium density:

$$n(T) = \frac{\Gamma}{\Lambda_{\rm low-metal}(x,T)} = \frac{10^{-40}{\rm J\cdot m^3\cdot s^{-1}}}{\Lambda_{\rm low-metal}(x,T)} \times 2\times10^7\ {\rm m^{-3}} \tag{1.2.9}$$

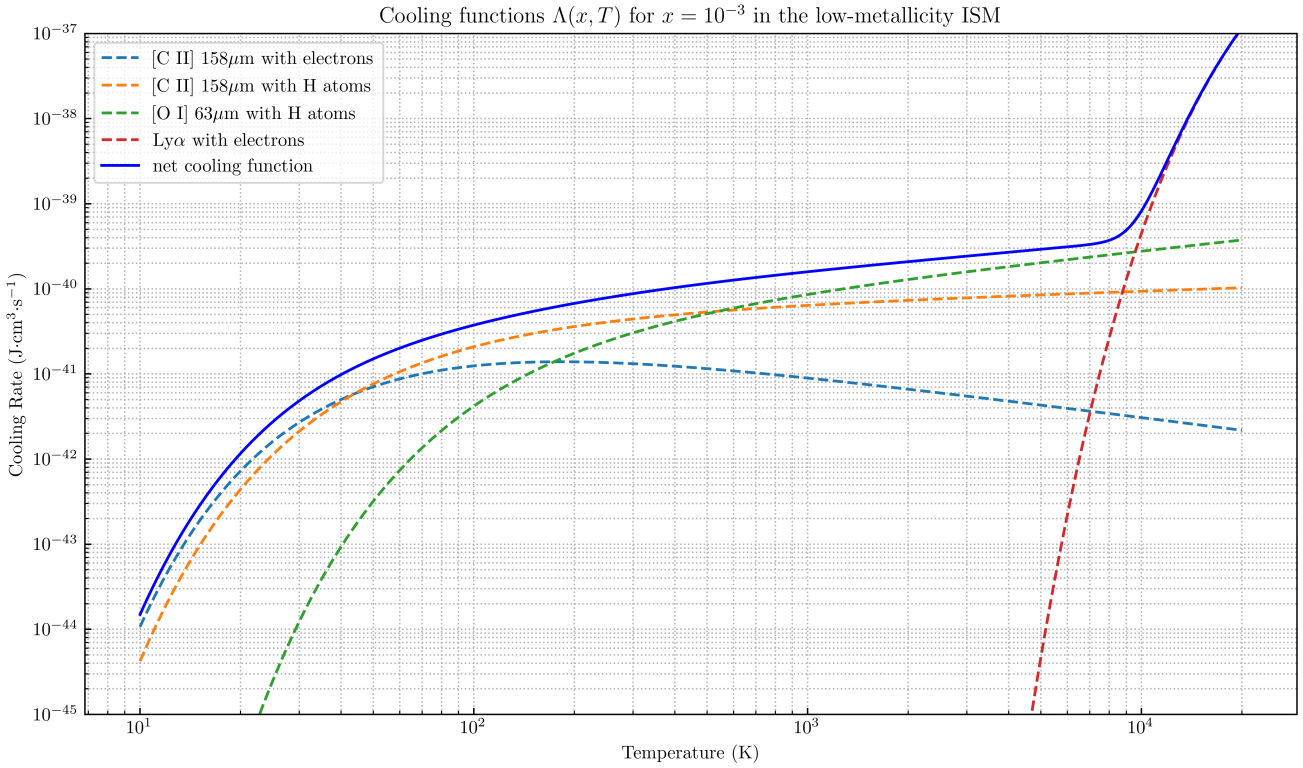

Figure 2: Cooling functions $\Lambda(x,T)$ for $x = 10^{-3}$ in the low-metallicity ISM

Plot $n(T)$ in the density-temperature plane (see Figure 3).

1.2.4

Plot and find the F-G-H points in the 2-phase ISM equilibrium diagram in the low-metallicity ISM. Locate possible temperature equilibrium points for pressure $p = 2 \times 10^{-13}$ dyn/cm^2. Comment on the role of gas metallicity in determining the properties of the stable phases of the ISM in a galaxy.

Solution: Substituting Equation 1.2.8, the pressure is given by the ideal gas law:

$$p(T) = n(T) k_{\rm B} T = \frac{\Gamma}{\Lambda_{\rm low-metal}} k_{\rm B} T \tag{1.2.10}$$

By plotting $p(T)$ versus T, we can find the possible temperature equilibrium points. Due to the reduced metallicity in the low-metallicity ISM (see Figure 4), the cooling function $\Lambda_{\rm low-metal}$ is significantly lower. This reduction in cooling efficiency means that the cooling curve does not intersect the heating rate Γ at the temperatures corresponding to points F, G, and H. Consequently, these equilibrium points are absent in the low-metallicity ISM. In contrast, the local ISM (with normal metallicity) has F-G-H points present. Higher metallicity leads to a more efficient cooling function $\Lambda_{\rm local}$, allowing the cooling curve to intersect the heating rate at multiple temperatures, including points F, G, and H.

Metals provide numerous energy levels that facilitate radiative transitions, enabling the gas to cool efficiently through emission lines. With only 10% of the local ISM's metal content, the low-metallicity ISM has fewer available transitions for cooling, leading to a less efficient cooling process. The diminished cooling shifts the 2-phase ISM equilibrium diagram upwards, reducing or eliminating intersections

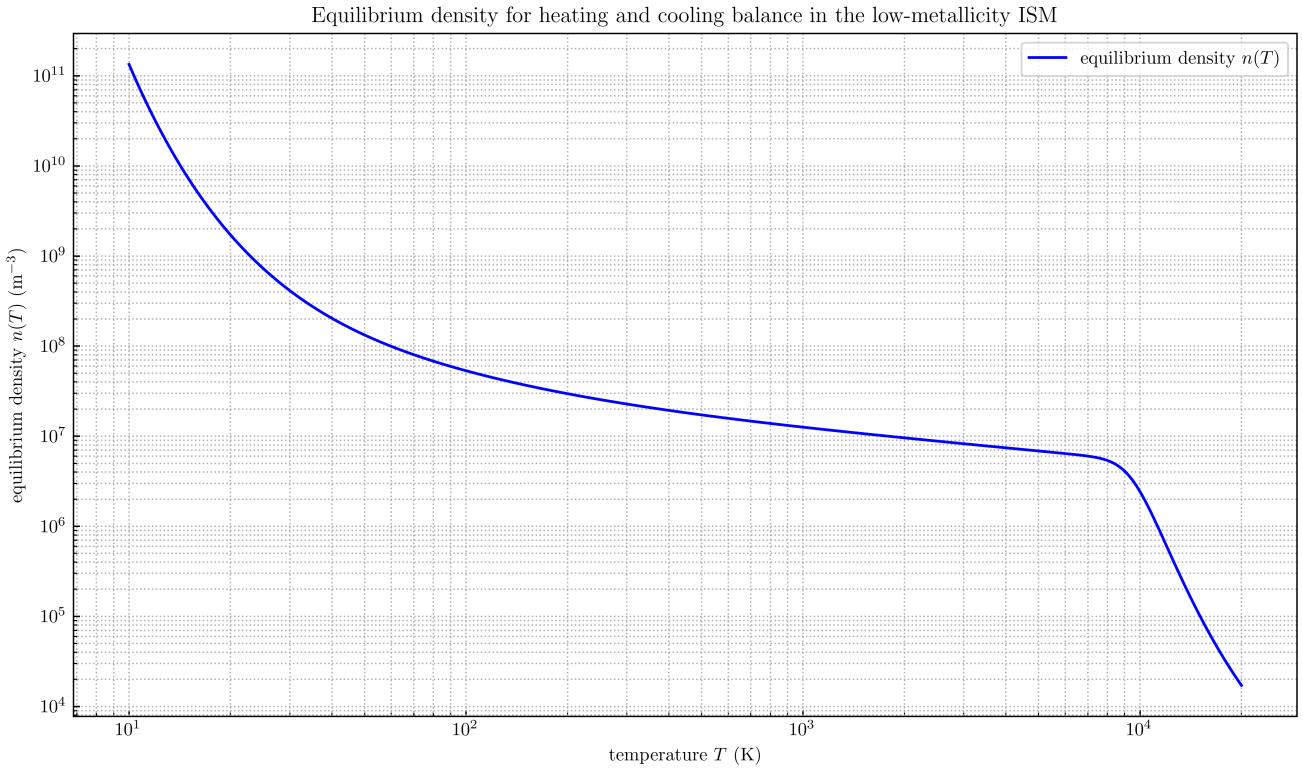

Figure 3: Equilibrium density for heating and cooling balance in the low-metallicity ISM

with certain pressure. Without these intersections, the ISM cannot achieve thermal equilibrium at the temperatures corresponding to points F, G, and H.

1.3

List all possible spectroscopic terms for electron configuration ...np^2 and ...np^3 and describe why.

Solution: For electron configuration ...np^2:

1. Orbital angular momentum coupling & total orbital angular momentum quantum number (L): Each electron in a p-orbital has an orbital angular momentum quantum number $l = 1$. For 2 electrons in p orbitals, the possible total orbital angular momentum values, L, are obtained by vector addition of the individual l values:

$$L = l_1 + l_2, l_1 + l_2 - 1, ..., |l_1 - l_2| = 2, 1, 0 \tag{1.3.1}$$

   These correspond to D, P, and S terms, respectively.

2. Spin angular momentum coupling & total orbital spin momentum quantum number (S): Each electron also has a spin quantum number $s = \frac{1}{2}$. For 2 electrons, the possible total spin values, S, are:

$$S = s_1 + s_2, s_1 + s_2 - 1, ..., |s_1 - s_2| = 1, 0 \tag{1.3.2}$$

   These correspond to $^{2S+1}$L $=^3$ L,^{1} L terms, respectively.

3. Pauli exclusion principle: The Pauli exclusion principle requires the total wave function of identical fermions (electrons) to be antisymmetric under their exchange. The total electronic wave function

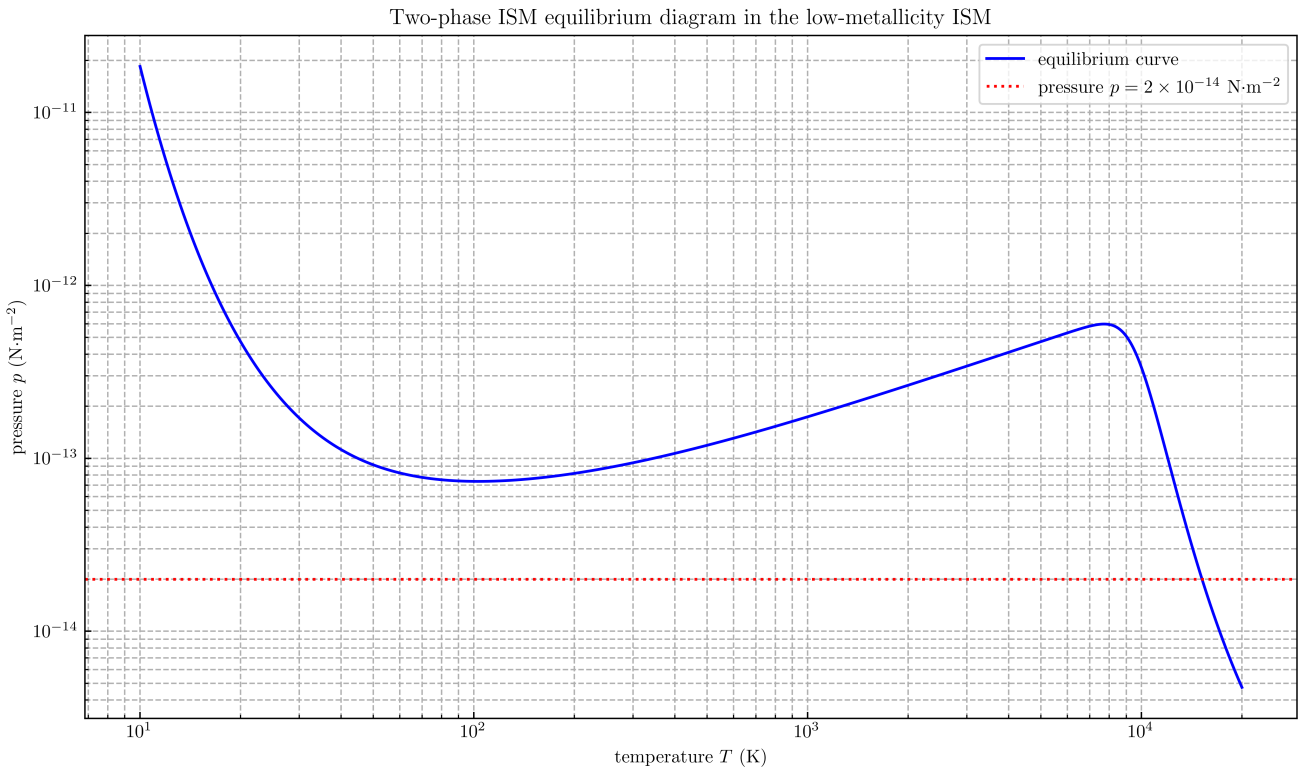

Figure 4: Two-phase ISM equilibrium diagram in the low-metallicity ISM

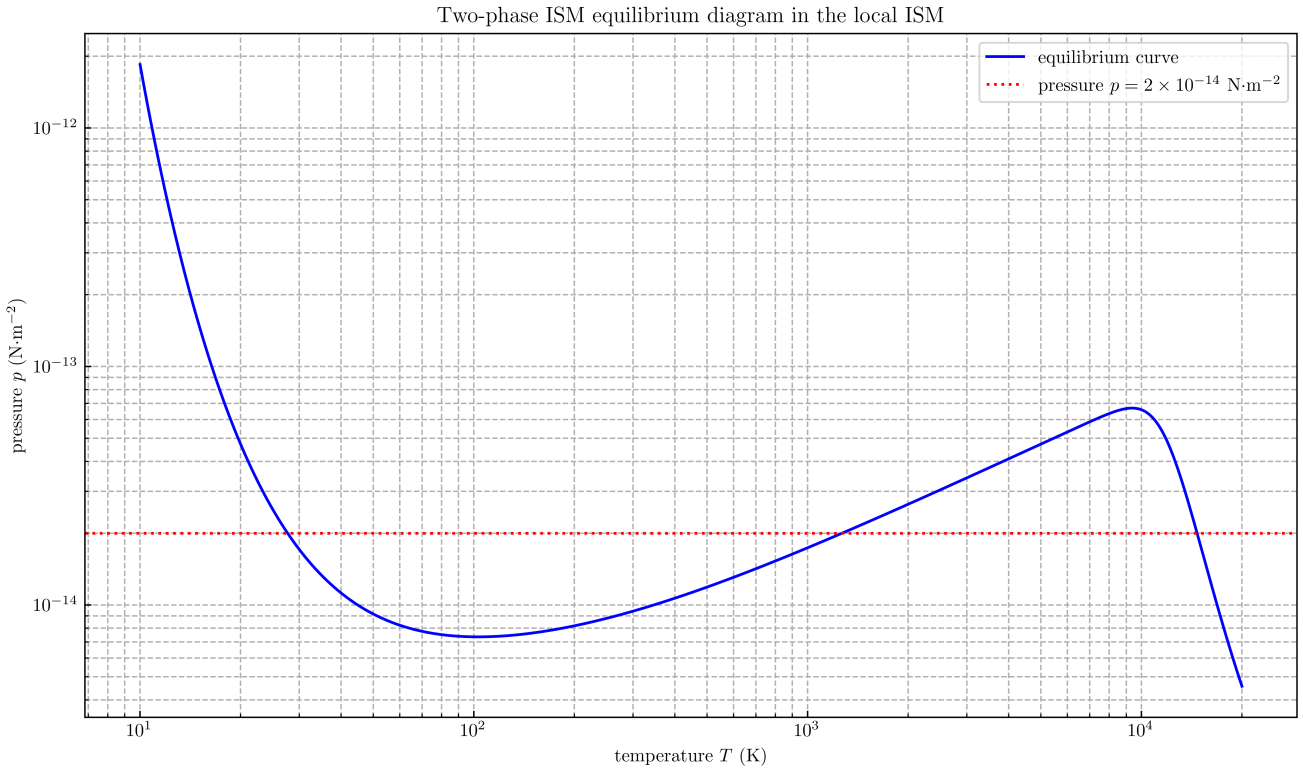

Figure 5: Equilibrium density for heating and cooling balance in the local ISM

is a product of the spatial (ψ_{space}) and spin (χ_{spin}) parts:

$$\Psi_{\text{total}} = \psi_{\text{space}} \cdot \chi_{\text{spin}} \tag{1.3.3}$$

If ψ_{space} (spatial part) is symmetric, then χ_{spin} (spin part) must be antisymmetric. If ψ_{space} is antisymmetric, then χ_{spin} must be symmetric. List the symmetry of spatial and spin functions:

- L = 0 (S term): symmetric spatial function (ψ^{+}_{space})
- L = 1 (P term): antisymmetric spatial function (ψ^{-}_{space})
- L = 2 (D term): symmetric spatial function (ψ^{+}_{space})
- S = 0 (^{1}L term): antisymmetric spin function (χ^{-}_{spin})
- S = 1 (^{3}L term): symmetric spin function (χ^{+}_{spin})

By combining the spin and spatial parts, the allowed terms for the system are ^{1}S,^{1} D,^{3} P.

4. Parity (p): The parity of a term is determined by the orbital angular momenta ls of the electrons. For the ...np^2 configuration, where $l = 1$ for each p-electron, the parity is:

$$p = (-1)^{l_1+l_2+\cdots} = (-1)^{1+1} = 1 \tag{1.3.4}$$

Thus, all allowed terms for the ...np^2 configuration have even parity: ^{1}S,^{1} D,^{3} P.

5. LS coupling & total angular momentum quantum number (J): The total angular momentum J is the vector sum of the total orbital angular momentum L and the total spin angular momentum S. For each allowed term, J can take values from $|L - S|$ to $L + S$ in integer steps:

$$J = L + S,\ L + S - 1, \ldots, |L - S| \tag{1.3.5}$$

Thus, the allowed spectroscopic terms for the ...np^2 configuration are:

- $S = 0, L = 0 \Rightarrow J = 0 \Rightarrow {}^1\text{S}_0$
- $S = 0, L = 2 \Rightarrow J = 2 \Rightarrow {}^1\text{D}_2$
- $S = 1, L = 1 \Rightarrow J = 0, 1, 2 \Rightarrow {}^3\text{P}_0,{}^3\text{P}_1,{}^3\text{P}_2$

For electron configuration ...np^3, the situation is similar:

- $s_1 = s_2 = s_3 = \dfrac{1}{2} \Rightarrow S = \dfrac{1}{2}, \dfrac{3}{2}$
- $l_1 = l_2 = l_3 = 1 \Rightarrow L = 0, 1, 2, 3$
- $l_1 = l_2 = l_3 = 1 \Rightarrow p = (-1)^{1+1+1} = -1$
- $S = \dfrac{3}{2}, L = 0 \Rightarrow J = \dfrac{3}{2} \Rightarrow {}^4\text{S}^{\text{o}}_{3/2}$

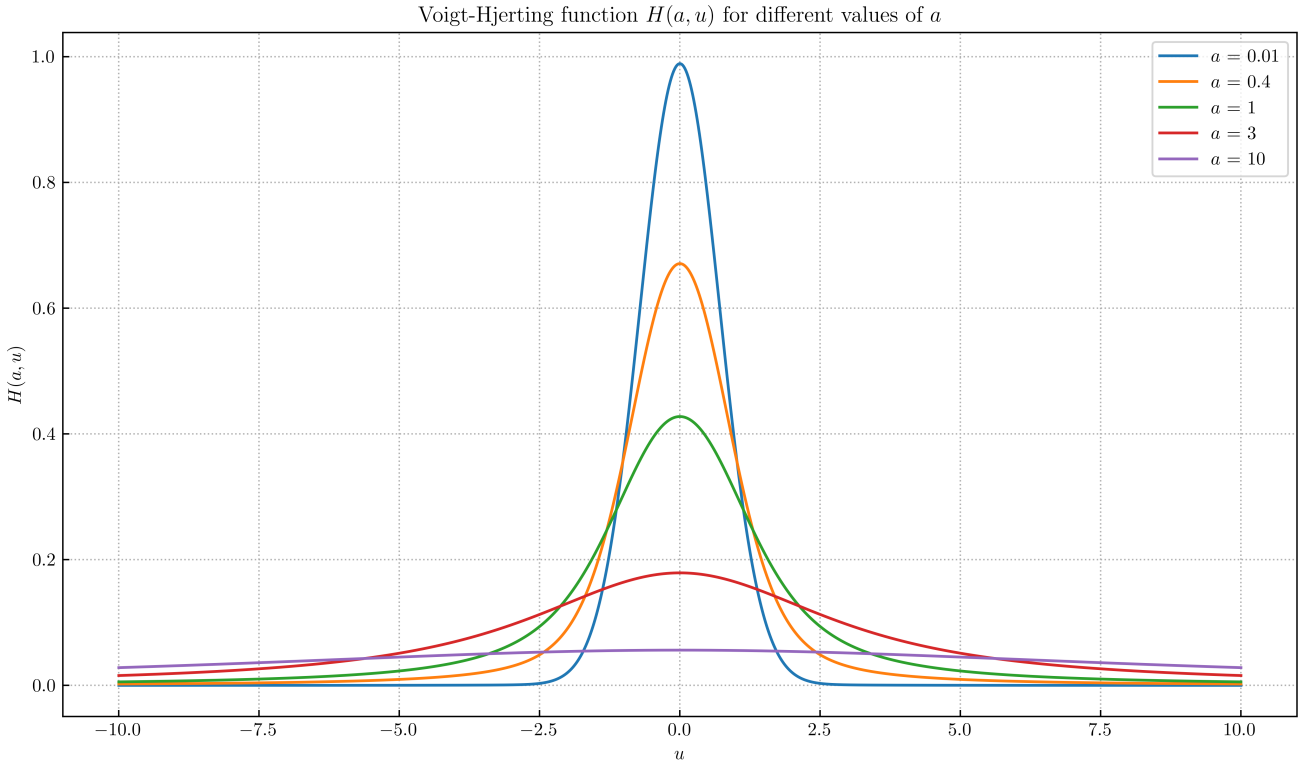

Figure 6: Voigt-Hjerting function for different values of a

- $S = \frac{1}{2}, L = 1 \Rightarrow J = \frac{1}{2}, \frac{3}{2} \Rightarrow {}^2\mathrm{P}^{\mathrm{o}}_{1/2}, {}^2\mathrm{P}^{\mathrm{o}}_{3/2}$
- $S = \frac{1}{2}, L = 2 \Rightarrow J = \frac{3}{2}, \frac{5}{2} \Rightarrow {}^2\mathrm{D}^{\mathrm{o}}_{3/2}, {}^2\mathrm{D}^{\mathrm{o}}_{5/2}$

1.4

Numerically integrate the Voigt-Hjerting function

$$H(a, u) = \frac{a}{\pi} \int_{-\infty}^{+\infty} \frac{e^{-y^2}}{(u - y)^2 + a^2} \mathrm{d}y \tag{1.4.1}$$

1.4.1

Plot $H(a, u)$ as a function of u for different a from 0 to 10.

Solution: See Figure 6.

1.4.2

Show that $H(a, u)$ has a Gaussian-like core and Lorentz-like wing and propose an approximate function form that simplifies the calculation of H and covers both regimes in the limit of $a \ll 1$.

Solution: We rewrite the Voigt-Hjerting function as the convolution of a Lorentz profile F and a Gauss

profile G:

$$H(a,u) = \int_{-\infty}^{+\infty} F(u-y)G(y)\mathrm{d}y \tag{1.4.2}$$

$$F(u) = \frac{1}{\pi}\frac{a}{u^2+a^2} \tag{1.4.3}$$

$$G(u) = e^{-u^2} \tag{1.4.4}$$

Observe that we can view Dirac δ function as a limit of a Gauss or a Lorentz function:

$$\delta(u) = \lim_{a\to 0}\frac{1}{\sqrt{\pi}a}e^{-u^2/a^2} = \lim_{a\to 0}\frac{1}{\pi}\frac{a}{u^2+a^2} \tag{1.4.5}$$

When $a \ll 1$, we can profitably expand the Voigt–Hjerting function in a Taylor series expansion around $a = 0$:

$$H(a,u) \approx H(0,u) + a\left.\frac{\mathrm{d}H(a,u)}{\mathrm{d}a}\right|_{a=0} \approx e^{-u^2} + \frac{a}{\sqrt{\pi}u^2} \tag{1.4.6}$$

where $H(0,u)$ and $a\left.\dfrac{\mathrm{d}H(a,u)}{\mathrm{d}a}\right|_{a=0}$ are calculated by:

$$\begin{aligned} H(0,u) &= \lim_{a\to 0}\int_{-\infty}^{+\infty} F(u-y)G(y)\mathrm{d}y = \int_{-\infty}^{+\infty}\lim_{a\to 0} F(u-y)G(y)\mathrm{d}y \\ &= \int_{-\infty}^{+\infty}\delta(u-y)G(y)\mathrm{d}y = G(u) = e^{-u^2} \end{aligned} \tag{1.4.7}$$

$$\begin{aligned} \frac{\mathrm{d}H(a,u)}{\mathrm{d}a} &= \frac{\mathrm{d}}{\mathrm{d}a}\int_{-\infty}^{+\infty} F(u-y)G(y)\mathrm{d}y = \int_{-\infty}^{+\infty}\frac{\partial F(u-y)}{\partial a}G(y)\mathrm{d}y \\ &= \int_{-\infty}^{+\infty}\frac{1}{\pi}\frac{(u-y)^2-a^2}{[(u-y)^2+a^2]^2}G(y)\mathrm{d}y \end{aligned} \tag{1.4.8}$$

$$\begin{aligned} a\left.\frac{\mathrm{d}H(a,u)}{\mathrm{d}a}\right|_{a=0} &= \int_{-\infty}^{+\infty}\frac{a}{\pi}\frac{1}{(u-y)^2}G(y)\mathrm{d}y = \int_{-\infty}^{+\infty}\frac{a}{\pi}\frac{1}{(u-x/a)^2}e^{-x^2/a^2}\frac{\mathrm{d}x}{a} \\ &\approx \int_{-\infty}^{+\infty}\frac{a}{\sqrt{\pi}}\frac{1}{(u-x/a)^2}\delta(x)\mathrm{d}x = \frac{a}{\sqrt{\pi}u^2} \end{aligned} \tag{1.4.9}$$

Here the central core of the line profile (small u) is well-approximated by treating the intrinsic line profile as a Dirac δ function, so that the central core of the line is the Gaussian core approximation, because the Lorentz function contributes minimally in the centre. In the wings (for large u), the Lorentz tail dominates. To combine the Gaussian-like core and Lorentzian-like wings, we propose the following approximate function that smoothly transitions between these two behaviours:

$$H_{\mathrm{approx}}(a,u) = \begin{cases} e^{-u^2} & |u| \leqslant u_0 \\ e^{-u^2} + \dfrac{a}{\sqrt{\pi}u^2} & |u| \geqslant u_0 \end{cases} \tag{1.4.9}$$

where u_0 satisfies:

$$\begin{aligned} e^{-u_0^2} &= \frac{a}{\sqrt{\pi}u_0^2} \\ \Leftrightarrow u_0^2 e^{-u_0^2} &= \frac{a}{\sqrt{\pi}} \end{aligned} \tag{1.4.10}$$

For $a = 0.01$, $u_0 \approx 101$.

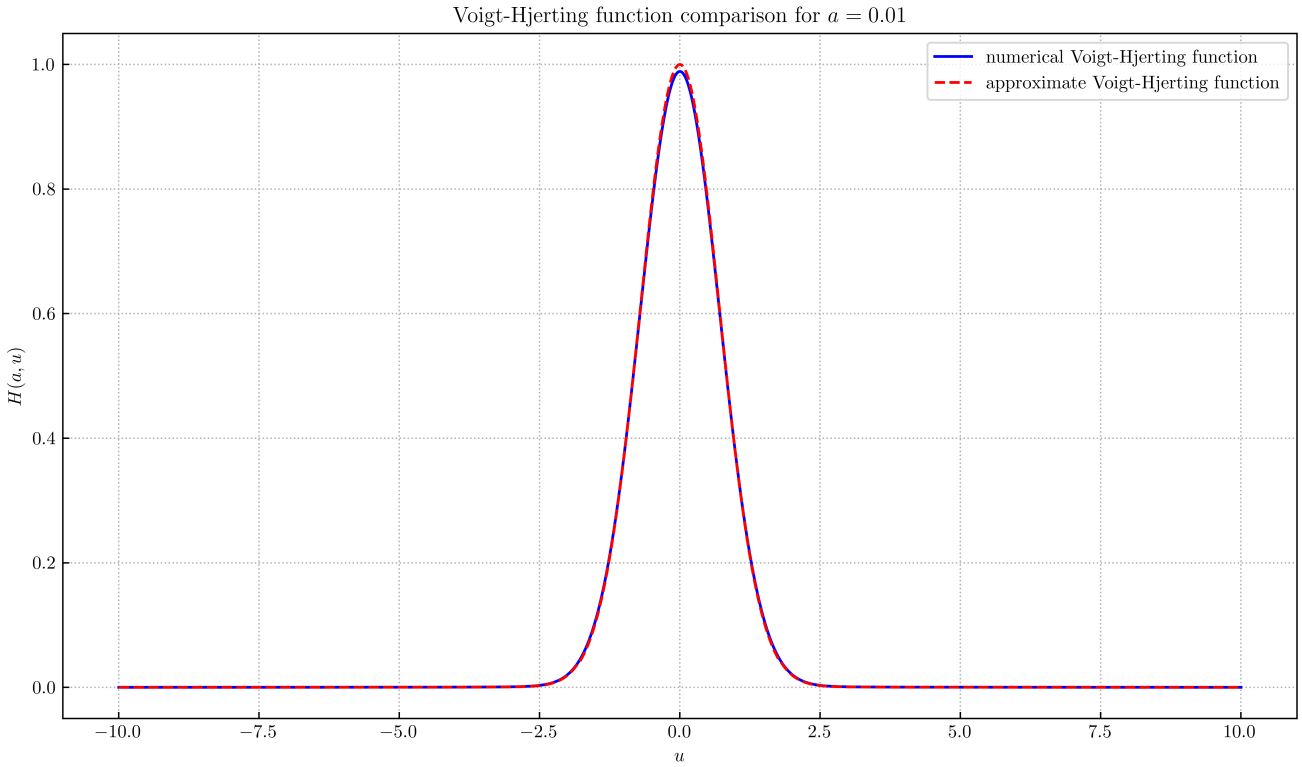

Figure 7: Voigt-Hjerting function comparison for $a = 0.01$

1.4.3

Overplot your proposed approximate function to the accurate numerical result and calculate the relative error of your function over u for $a = 0.01$.

Solution: The relative error ε between the numerical Voigt-Hjerting function $H(a, u)$ and the approximate Voigt function $H_{\text{approx}}(a, u)$ is given by:

$$\varepsilon = \frac{|H_{\text{approx}}(a, u) - H(a, u)|}{H(a, u)} \tag{1.4.11}$$

See Figure 7 and Figure 8.

1.5 -2

A distant quasar at a redshift $z_{\text{q}} = 2.5$ is observed on a line-of-sight which passes through the disk of an intervening galaxy. A strong absorption feature is observed in the continuum spectrum of the quasar at an observed wavelength of 3647 Å. This absorption feature is interpreted as Lyα absorption in the intervening galaxy, implying that the galaxy is at a redshift $z_{\text{g}} = 2.0$.

1.5.1

The absorption feature at 3647 Å has an observed equivalent width $W_\lambda = 6.0$ Å. The equivalent width that would be observed by an observer in the rest-frame of the absorbing galaxy would be $W_{\lambda,\text{g}} = \dfrac{6.0\,\text{Å}}{1 + z_{\text{g}}} = 2.0$ Å. Estimate the HI optical depth at line-center of the Lyα line which is required to produce this equivalent width. Assume the 1D velocity dispersion of the HI $b = 20$ km/s. b=sqrt(2)*20,(eq 9.7 in Draine,2011)

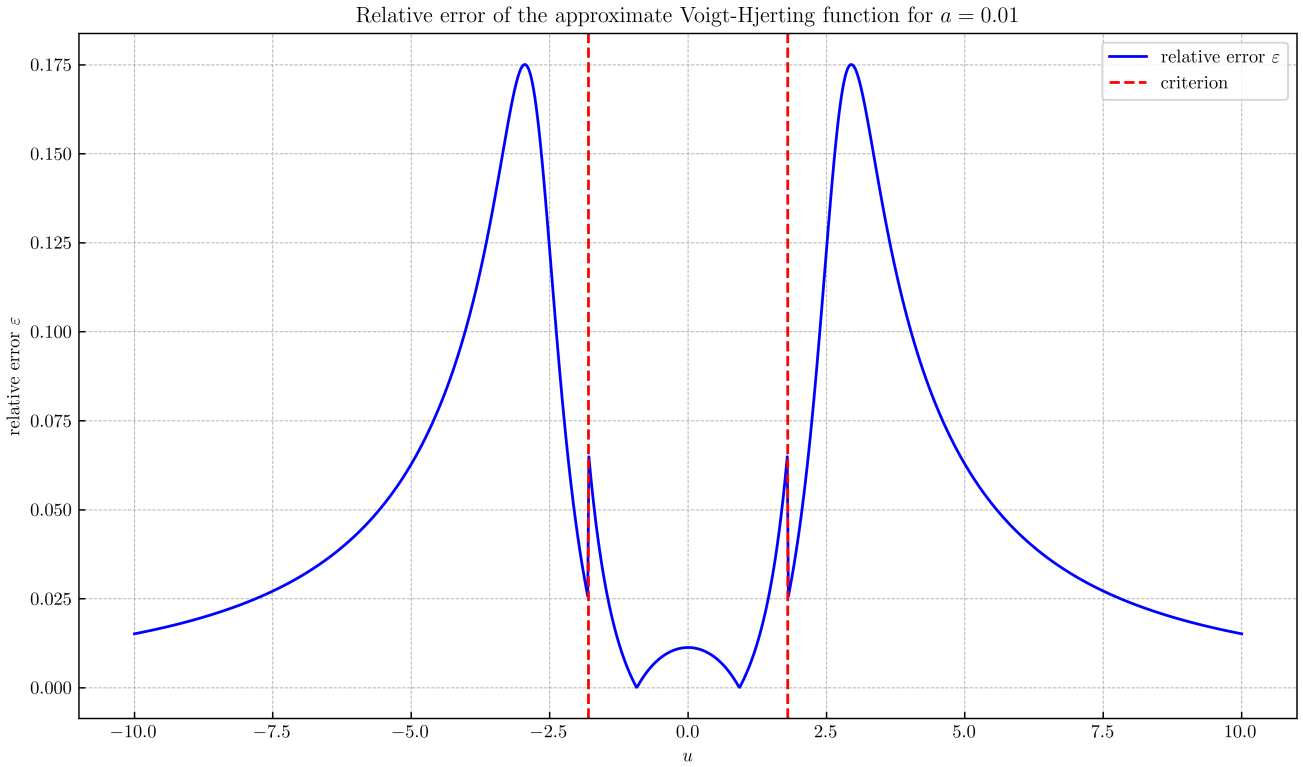

Figure 8: Relative error of the approximate Voigt-function for $a = 0.01$

Solution: For the linear part of the curve of growth, where the optical depth at the line center $\tau_0 < 1$, the equivalent width W_λ can be calculated as:

$$W_{\lambda,\mathrm{g}} = \frac{\sqrt{\pi} b}{c} \lambda_0 \tau_0 \tag{1.5.1}$$

Thus, we obtain τ_0 as:

$$\tau_0 = \frac{c W_{\lambda,\mathrm{g}}}{\sqrt{\pi} b \lambda_0} \approx 13.91 > 1 \tag{1.5.2}$$

Since $\tau_0 > 1$, this is not in the linear part of the curve. Next, assuming we are in the flat part of the curve, we have:

$$W_{\lambda,\mathrm{g}} = \frac{2b}{c} \lambda_0 \sqrt{\ln \tau_0} \tag{1.5.3}$$

$$\Rightarrow \tau_0 = \exp\left(\frac{c^2 W_{\lambda,\mathrm{g}}^2}{4 b^2 \lambda_0^2}\right) \approx 1.07 \times 10^{66} > \tau_{\mathrm{damp}} \tag{1.5.4}$$

For the Lyα line, the damping optical depth is given by:

$$\tau_{\mathrm{damp}} \approx 455 \left(\frac{b}{1\ \mathrm{km\ s^{-1}}}\right) \left[1 + 0.2 \ln\left(\frac{b}{1\ \mathrm{km\ s^{-1}}}\right)\right] \approx 1.455 \times 10^4 \tag{1.5.5}$$

For Ly-α absorption, $\gamma_{ul} = 4.7 \times 10^8\ \mathrm{s}^{-1}$. Now, we compute the square-root term for $W_{\lambda,\mathrm{g}}$:

$$W_{\lambda,\mathrm{g}} = \lambda_0 \sqrt{\frac{b \gamma_{ul} \tau_0}{\sqrt{\pi} c \nu_{ul}}} = \frac{\lambda_0}{\pi^{1/4} c} \sqrt{\lambda_0 b \gamma_{ul} \tau_0} \tag{1.5.6}$$

$$\Rightarrow \tau_0 = \frac{\sqrt{\pi} c^2 W_{\lambda,\mathrm{g}}^2}{b \lambda_0^3 \gamma_{ul}} \approx 3.773 \times 10^5 \tag{1.5.7}$$

1.5.2

What is the column density of HI in the $n = 1$ level in the intervening galaxy? Remark on the similarity/difference between the ISM of this galaxy vs. the local ISM in our Galaxy.

Solution: Column density can be calculated as:

$$n_l = 1.9 \times 10^{22}\ \mathrm{m}^{-2} \left(\frac{W_{\lambda,\mathrm{g}}}{1\text{Å}} \right)^2 \approx 7.6 \times 10^{22}\ \mathrm{m}^{-2} \tag{1.5.8}$$

In the Milky Way, typical HI column densities through the disk are on the order of $n_l(\mathrm{HI}) \approx 10^{25}\mathrm{m}^{-2}$ or higher. The column density calculated for the intervening galaxy is about two orders of magnitude lower. This suggests that the ISM in the intervening galaxy along this line of sight is less dense than in our Galaxy. Possible reasons include:

- The line of sight passes through a less dense region of the galaxy (e.g., above the galactic plane or through a region with less gas).
- The intervening galaxy may be at an earlier stage of evolution, with less accumulated gas and dust.
- Differences in galaxy type (e.g., a dwarf galaxy vs. a spiral galaxy like the Milky Way).